

Spherically symmetric potential for $\text{Ar}(^3P_{2,0}) + \text{N}_2(X)$ from velocity-dependent total scattering cross sections

K. A. Hardy and J. W. Sheldon

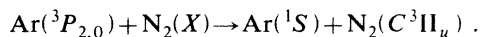
Physics Department, Florida International University, Miami, Florida 33199

(Received 30 June 1986; revised manuscript received 30 September 1987)

Total scattering cross sections for the $\text{Ar}(^3P_{2,0}) + \text{N}_2(X)$ are reported over a relative velocity range from 0.55 to 1.75 km/s. The data are compared with cross sections calculated from a spherically symmetric potential with four adjustable parameters. The best fit gave r^{-5} and r^{-6} potential constants of 6.7 ± 1.2 and 37.8 ± 11.6 a.u., respectively.

I. INTRODUCTION

Argon-nitrogen gas mixtures are used for producing gas lasers,¹⁻³ and argon metastables are of prime importance in energy-disposal schemes of these systems.^{3,4} Experiments by Muschlitz and co-workers,^{5,6} Krenos and Bruno,⁷ Martin and co-workers,^{8,9} and the theoretical work of Gislason, Kleyn, and Los¹⁰ have identified the vibrational branching ratios in the electron energy transfer process



More recently Nguyen and Sadeghi¹¹ have state selected the metastables in observing this process. Yet, there are some questions concerning the $\text{Ar}(^3P_{2,0}) + \text{N}_2(X)$ interaction potential.

The $\text{Ar}(^3P_{2,0}) + \text{N}_2(X)$ system was investigated by Winicur and Fraites¹² in a crossed-beam measurement of the differential scattering cross section at a single-collision energy from which they obtained a spherically symmetric potential. Their results, which are discussed in detail in Sec. IV indicate that the inverse r^{-6} attractive potential is 20 times less than theoretical, and the overall potential curve is considerably different from that obtained for the electronically similar $\text{K} + \text{N}_2$ system.^{13,14} This provided the motivation for the total cross-section measurements reported here.

II. EXPERIMENTAL PROCEDURE

The single-beam machine used in this work has been described earlier.^{15,16} Briefly, it consists of a gas discharge beam source of metastable argon atoms which are collimated, chopped, and velocity analyzed by the time-of-flight method. The beam velocity resolution as calculated from the beam and chopper geometry varies from 1.2% at a relative velocity of 0.5 km/s to 4.2% at 1.74 km/s. The relative velocity-dependent total cross sections were obtained from measured beam velocity-dependent effective cross sections by averaging over the target gas velocity distribution (at 27°C) following Lang, Lilenfeld, and Kinsey.¹⁷ This procedure neglects the effect of glory oscillations, a point which is discussed further in Sec. IV.

No separation of the two metastable states was at-

tempted, however, in another work¹⁸ with a similar gas discharge source 3P_2 states were shown to dominate by about 6 to 1 over the 3P_0 . The beam geometry has an angular resolution by the Kusch criterion¹⁹ of 1.8 minutes which is sufficient to ensure that small-angle scattering errors in the observed total scattering cross sections are negligible.²⁰ The target gas pressure was measured with an electronic capacitance manometer. A computer controlled the data-acquisition procedure, cycled the target gas in and out of the collision cell, and thereby averaged out long-term drift in the beam intensity.

The measured cross sections are compared with values calculated for an assumed potential form with adjustable parameters. The parameters were adjusted by a non-linear least-squares procedure to minimize the χ^2 between the calculated and measured cross sections. When a minimum χ^2 was reached by varying all the free parameters, the process was repeated with a new set of starting parameters until a true minimum was reached. Each calculated cross section was obtained from phase shifts computed by direct integration of the Schrödinger equation using the Numerov algorithm.²¹ The integration began at a point well inside the repulsive core where the wave function could be set equal to zero and went outward until the phase shift converged to within 0.1% of a constant value.

III. RESULTS

The $\text{Ar}^* + \text{N}_2$ total cross-section data are presented in Fig. 1. The log-log plot allows an estimate of the long-range r dependence of the interaction potential, since it is well known²⁰ that an r^{-s} -dependent potential leads to a mean slope of $2/(s-1)$ on such a plot. While the present measurements are absolute cross sections, they are displayed in Fig. 1 in arbitrary units. This allows comparison with relative total scattering cross-section data obtained some time ago for the electronically similar $\text{K} + \text{N}_2$ system.²² For the $\text{K} + \text{N}_2$ case the slope of 0.4 indicates a long-range van der Waals r^{-6} potential.

We have previously reported excellent agreement with experimental results from other laboratories for $\text{He}^* + \text{Kr}$, Xe (Ref. 23), and Ne^* and $\text{Ar}^* + \text{He}$ (Ref. 24). In these interactions the dominant long-range interaction is the van der Waals r^{-6} term and the similarity to the electronically analogous alkali-metal-rare-gas collisions

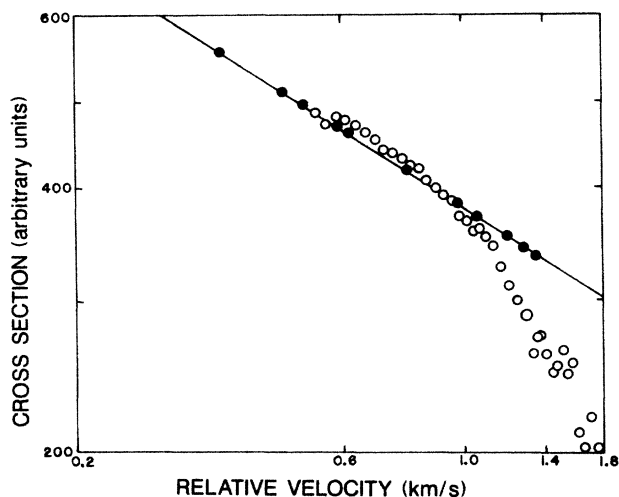


FIG. 1. Comparison of present results with those of the $K+N_2$ system; open circles, present results; closed circles, Ref. 22. The relative cross sections are normalized to the lowest velocity data point.

was demonstrated. The Ar^*+N_2 case differs from $K+N_2$ since both Ar^* and N_2 have quadrupole moments. We have used a potential of the form

$$V(r) = \epsilon \left[\left(\frac{f+5}{n-5} \right) \left(\frac{r_m}{r} \right)^n - \frac{n(1-f)+6f}{n-5} \left(\frac{r_m}{r} \right)^5 - f \left(\frac{r_m}{r} \right)^6 \right] \quad (1)$$

since there is reason to believe there is an r^{-5} quadrupole-quadrupole interaction term. Here the well depth $-\epsilon$ occurs at r_m , and f is a mixing parameter varying between 0 and $n/(n-6)$ as the long-range potential goes from pure r^{-5} to pure r^{-6} dependence. Adjusting n , ϵ , r_m , and f for a best fit of the computed cross sec-

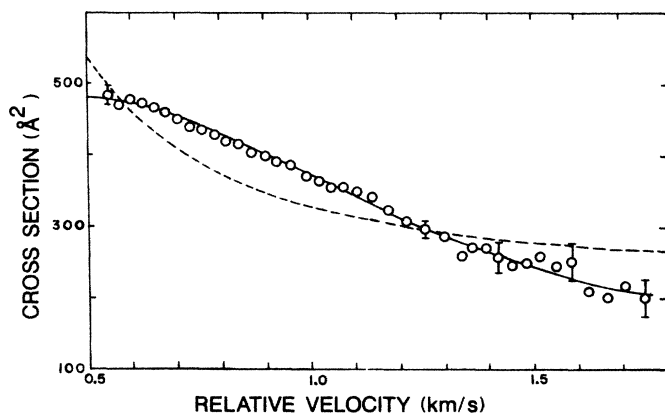


FIG. 2. Measured Ar^*+N_2 total cross sections compared to solid curve calculated from Eq. (1) with $n=10$, $f=0.83$, $\epsilon=8.13 \times 10^{-5}$ a.u., and $r_m=9.08$ a.u., dashed curve calculated from Eq. (2) with $M=16$, $N=24$, $P=12$, $\epsilon=3.69 \times 10^{-5}$ a.u., and $r_m=12.62$ a.u.

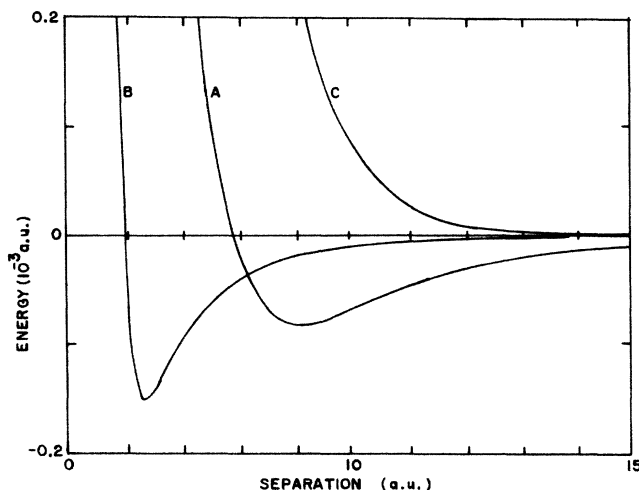


FIG. 3. Potential energy: curve A, present result for Ar^*+N_2 ; curve B, result of Ref. 12 for Ar^*+N_2 ; curve C, result of Ref. 14 for $K+N_2$.

tions to the absolute experimental values gave the result presented in Fig. 2, where a linear plot is used to emphasize accuracy of the data and goodness of fit. The best-fit potential parameters are presented in Table I where they are compared with other work. The uncertainties in the present results represent the range of parameters which produce calculated cross sections within the experimental error bars.

The potential curves for the Ar^* and $K+N_2$ systems are presented in Fig. 3. The $K+N_2$ curve is an exponential repulsion form obtained experimentally by Malerich, Povodator, and Cross¹⁴ for high-collision energy (1–1000 eV).

IV. DISCUSSION

In the present work it is assumed that the Ar^*+N_2 total scattering cross sections is the same as the elastic scattering cross section. This is justified since the quenching cross sections for these collisions⁹ are within our reported error bars.

In atom-molecule collisions rotational excitation can occur due to deviations of the interaction potential from spherical symmetry. Anisotropy has been observed in $K+N_2$ differential scattering measurements,^{26–28} however, only close encounters with the repulsive core exhibited the effect. The present measurements are primarily influenced by the long-range potential. Furthermore, in $Ar(1S)+N_2(X)$ collisions the glory structure was not affected, and a spherically averaged potential model was quite satisfactory.²⁹

A substantial difference is shown in Fig. 1 between the velocity dependence of $K+N_2$ and Ar^*+N_2 cross sections. The steep decline of the Ar^*+N_2 data for speeds above $0.4\epsilon r_m/\hbar \cong 1$ km/s is typical for the normal low-to-high velocity transition.³⁰ The decline may simply mark the transition region of this system and have nothing necessarily to do with a r^{-5} long-range interaction. Thus it seemed reasonable to try to fit the present data with the modified Lennard-Jones potential form

TABLE I. Potential parameters (measured in au.).

System	n	f	$10^5\epsilon$	r_m	C_5	C_6	Source
Ar* + N ₂	10 ^a	0.83±0.20	8.13±0.15	9.08±0.05	6.7±1.2 ^b	37.8±11.6 ^b	Present Experiment (Ref. 12)
	24		15.0	6.31		11.1 ^c	
K + N ₂						299 ^d	Theory Experiment (Ref. 13)
						250	
						286 ^d	Theory

^aOnly integers were considered.

^bFrom Eq. (1).

^cFrom the double Lennard-Jones potential (Ref. 12), $C_6 = (\frac{20}{17})\epsilon r_m^6$.

^dFrom the Kramer-Herschbach rule (Ref. 25).

$$V(M, P; N, 6) = \begin{cases} \frac{\epsilon P}{(M-P)} \left[\left(\frac{r_m}{r} \right)^M - \frac{M}{P} \left(\frac{r_m}{r} \right)^P \right], & r \leq r_m \\ \frac{6\epsilon}{(N-6)} \left[\left(\frac{r_m}{r} \right)^N - \frac{N}{6} \left(\frac{r_m}{r} \right)^6 \right], & r \geq r_m \end{cases} \quad (2)$$

which was used by Winicur and Fraites.¹² The best fit for this potential, which is compared with the measurements in Fig. 2, was not acceptable.

A repulsive quadrupole-quadrupole long-range interaction, which in principle is possible,³¹ could explain why the C_6 value obtained in the curve fitting was too low. However, in several attempts to fit the measured data using Eq. (1), but starting with a positive value of the r^{-5} term, the curve-fitting program consistently sought negative values to minimize χ^2 .

The use of the procedure of Lang, Lilenfeld, and Kinsey¹⁷ to convert the measured effective cross sections $Q_e(v_1)$ (where v_1 is the beam velocity) to the average relative velocity-dependent total cross sections $Q(\bar{g})$ can be questioned, since it neglects the influence of glory oscillations.

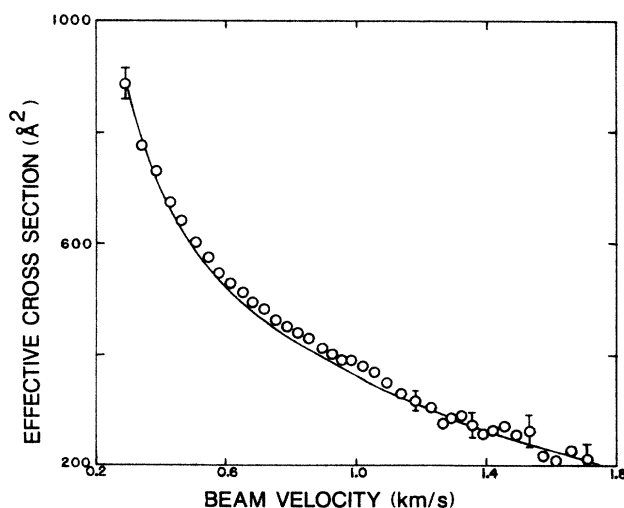


FIG. 4. Measured Ar* + N₂ effective sections compared to the curve calculated from Eq. (3).

As a check on this procedure we have computed $Q_e(v_1)$ using

$$Q_e(v_1) = \frac{1}{\sqrt{\pi} v_2 v_1^2} \int_0^\infty Q(g) g^2 (E^- - E^+) dg, \quad (3)$$

where

$$E^\mp = \exp \left[- \left(\frac{v_1 \mp g}{v_2} \right)^2 \right],$$

v_2 is the most probable velocity of the N₂ target, and $Q(g)$ is calculated numerically from the potential (1) using the parameters given in the first row of Table I. The results are compared with the measured effective cross sections in Fig. 4. There is slight ($\sim 6\%$) systematic deviation of the data from the calculated values, but the deviation is within experimental error.

While the procedure of fitting theoretical cross sections to experimental values using an assumed interaction potential form does not yield a unique potential, it does seem from the presentations in Figs. 1 and 2 that our data shows the potential for the Ar* + N₂ system to contain r^{-5} and r^{-6} long-range interaction terms. The r^{-5} quadrupole-quadrupole interaction term is expected for P -state atom encounters with homonuclear diatomic molecules, since both have quadrupole moments.^{31,32}

V. CONCLUSIONS

The Ar* + N₂ total elastic scattering cross section can be described by a spherically symmetric potential that differs substantially from the K + N₂ potential. The Ar* + N₂ system exhibits some effect of the r^{-5} quadrupole-quadrupole long-range interaction. Both our work and that of Winicur and Fraites¹² indicate the van der Waals constant for Ar* + N₂ to be an order of magni-

tude less than the $K + N_2$ system or the $Ar^* + N_2$ value based on polarizabilities and the Slater-Kirkwood formula. We offer no theoretical explanation for this difference, however, we are not the first to observe it. The C_6 value measured by Winicur and Fraites¹² for $Ar^* + N_2$ is three times smaller than the present result. Both works also indicate the repulsive core for $Ar^* + N_2$ to be smaller than for $K + N_2$.

ACKNOWLEDGMENTS

It is a pleasure to acknowledge the advice and encouragement that we received from Professor E. E. Muschlitz, Jr., of the University of Florida. The authors are also very grateful to Professor E. A. Mason for suggesting the possibility of the r^{-5} potential term playing a role in the $Ar^* + N_2$ interaction.

-
- ¹M. S. Chou and G. A. Zawadzkas, *IEEE J. Quantum Electron.* **17**, 77 (1981).
- ²P. Polak-Dingels and N. Djeu, *J. Appl. Phys.* **54**, 6818 (1983).
- ³C. H. Chen, M. G. Payne, G. S. Hurst, and J. P. Judish, *J. Chem. Phys.* **65**, 4028 (1976).
- ⁴J. V. Bozin, V. V. Urošević, and Z. Lj. Petrović, *Z. Phys. A* **312**, 349 (1983).
- ⁵E. R. Cutshall and E. Muschlitz, Jr. *J. Chem. Phys.* **70**, 3171 (1979).
- ⁶A. N. Schweid, M. A. D. Fluendy, and E. E. Muschlitz, Jr., *Chem. Phys. Lett.* **42**, 103 (1976).
- ⁷J. Krenos and J. Bel Bruno, *J. Chem. Phys.* **65**, 5017 (1976).
- ⁸W. Lee and R. M. Martin, *J. Chem. Phys.* **63**, 962 (1975).
- ⁹T. P. Parr and R. M. Martin, *J. Chem. Phys.* **69**, 1613 (1978).
- ¹⁰E. A. Gislason, A. W. Kleyn, and J. Los, *Chem. Phys. Lett.* **67**, 252 (1979).
- ¹¹T. D. Nguyen and N. Sadeghi, *Chem. Phys.* **79**, 41 (1983).
- ¹²D. H. Winicur and J. L. Fraites, *J. Chem. Phys.* **61**, 1548 (1974).
- ¹³E. W. Rothe and R. B. Bernstein, *J. Chem. Phys.* **31**, 1619 (1959).
- ¹⁴C. J. Malerich, J. B. Povodator, and R. J. Cross, Jr. *Chem. Phys.* **20**, 409 (1977).
- ¹⁵K. A. Hardy and J. W. Sheldon, *Rev. Sci. Instrum.* **52**, 1802 (1981).
- ¹⁶J. W. Sheldon and K. A. Hardy, *Phys. Lett.* **98A**, 332 (1983).
- ¹⁷N. C. Lang, H. V. Lilienfeld, and J. L. Kinsey, *J. Chem. Phys.* **55**, 3114 (1971).
- ¹⁸M. E. Gersh, G. D. Sides, S. Y. Tang, and E. E. Muschlitz, Jr., *J. Appl. Phys.* **44**, 5356 (1973).
- ¹⁹P. Kusch, *J. Chem. Phys.* **40**, 1 (1964).
- ²⁰H. S. W. Massey, *Electronic and Ionic Impact Phenomena* (Oxford University, London, 1971), Vol. III.
- ²¹R. J. Munn, E. A. Mason, and F. J. Smith, *J. Chem. Phys.* **41**, 3978 (1964).
- ²²H. Pauly, *Z. Naturforsch* **15A**, 277 (1960).
- ²³K. A. Hardy and J. W. Sheldon, *Phys. Rev. A* **30**, 2761 (1984).
- ²⁴J. W. Sheldon and K. A. Hardy, *Phys. Rev. A* **33**, 731 (1986).
- ²⁵H. L. Kramer and D. R. Herschback, *J. Chem. Phys.* **53**, 2792 (1979).
- ²⁶D. Beck, V. Ross, and W. Schepper, *Z. Phys. A* **293**, 107 (1979).
- ²⁷W. Schepper, V. Ross, and D. Beck, *Z. Phys. A* **290**, 131 (1979).
- ²⁸D. Beck, V. Ross, and W. Schepper, *Phys. Rev. A* **19**, 2173 (1979).
- ²⁹B. Brunetti, G. Luzzati, F. Pirani, and G. G. Volpi, *J. Chem. Phys.* **79**, 273 (1979).
- ³⁰H. Pauly, in *Atom-Molecule Collision Theory*, edited by R. B. Bernstein (Plenum, New York, 1979).
- ³¹J. K. Knipp, *Phys. Rev.* **53**, 734 (1938).
- ³²J. O. Hirschfelder, C. F. Curtiss, and R. B. Bird, *Molecular Theory of Gases and Liquids* (Wiley, New York, 1967), p. 1013.